INTERNATIONAL JOURNAL FOR NUMERICAL METHODS IN ENGINEERING
Int. J. Numer. Meth. Engng. **43**, 195–219 (1998)

IMPLICIT CONSTITUTIVE MODELLING FOR VISCOPLASTICITY USING NEURAL NETWORKS†

TOMONARI FURUKAWA* AND GENKI YAGAWA

Department of Quantum Engineering and Systems Science, University of Tokyo 7-3-1 Hongo, Bunkyo-ku, Tokyo 113, Japan

ABSTRACT

Up to now, a number of models have been proposed and discussed to describe a wide range of inelastic behaviours of materials. The fatal problem of using such models is however the existence of model errors, and the problem remains inevitably as far as a material model is written explicitly. In this paper, the authors define the implicit constitutive model and propose an implicit viscoplastic constitutive model using neural networks. In their modelling, inelastic material behaviours are generalized in a state-space representation and the state-space form is constructed by a neural network using input–output data sets. A technique to extract the input–output data from experimental data is also described. The proposed model was first generated from pseudo-experimental data created by one of the widely used constitutive models and was found to replace the model well. Then, having been tested with the actual experimental data, the proposed model resulted in a negligible amount of model errors indicating its superiority to all the existing explicit models in accuracy. © 1998 John Wiley & Sons, Ltd.

KEY WORDS: implicit constitutive modelling; viscoplasticity; plasticity; neural networks

1. INTRODUCTION

There has been an accelerating rate at which various solids and structures were developed to assist the objective of industrial designers. In many industrial fields, they are often used under severe operating conditions such as cyclic loading, high-temperature, high-pressure and high irradiation, for instance, if they are used as pressure vessels and pipes of a nuclear plant. This gives rise to the necessity for inelastic analysis of materials, properties of which are characterized by material models or constitutive equations, based on the observation of simple experiments (tension, compression, torsion, etc.).

Because of the complexity of material behaviour, a great number of inelastic constitutive models have been developed accordingly.[1–8] Inelastic material models proposed so far can be classified into two types.[9] In the first type, the model is expressed only in terms of observable variables, although it is limited in its descriptive ability.[10] The second type of model has not only observable variables but also variables representing material internal behaviours.[2,3,11–13] Due to

* Correspondence to: Tomonari Furukawa, Department of Quantum Engineering and Systems Science, University of Tokyo, 7-3-1 Hongo, Bunkyo-ku, Tokyo 113, Japan. E-mail: tomonari@q.t.u-tokyo.ac.jp
† This paper was partially presented at XIXth International Congress of Theoretical and Applied Mechanics, Kyoto, in August 1996

CCC 0029–5981/98/020195–25$17.50

Received 14 July 1997
Revised 23 January 1998

the introduction of additional variables, this type of model has a larger degree-of-freedom in description, thus being superior to the first type.

The significant problem involved with such models is however that the models contain errors inevitably, as they are based on simple phenomenological investigations of material properties while real behaviours of material is very complex. Up to now, researchers rather have attempted to overcome this problem by either introducing higher-performance models or better parameter identification techniques.[14–18] However, they do not tackle the substance of the problem since any model is limited by the capability of their mathematical description, i.e. the model is written explicitly. On the other hand, a non-explicit approach appeared in the research by Ghaboussi *et al.*[19] and their subsequent papers, although their approach could not represent material behaviours accurately.

Therefore, in this paper, the authors first define the implicit constitutive model in contrast to all conventional constitutive models, and then propose an implicit viscoplastic model using neural networks based on the state-space method. The implicit model can describe material behaviours broadly without any heuristic determination of phenomenological formulations as it is constructed only from experimental data.[20,21] The state-space representation of the proposed technique enables the description of dynamical or viscoplastic behaviours of materials, and the use of neural networks as a universal function approximator allows us to simulate the behaviours accurately.

The next section deals with the fundamentals of neural networks, followed by a brief introduction to viscoplastic models in Section 3. In section 4, the implicit constitutive model is first defined, and then an implicit viscoplastic model is generalised in a state space form. Finally, a neural network constitutive model based on the state-space form is proposed. A simple technique to extract training data from experimental data is also described so that the proposed model can be used for the actual material data. Section 5 refers to numerical examples in order to investigate the performance of the proposed model. First, the capability of the proposed model to emulate one of the commonly used conventional models is investigated, and the proposed model is then tested with actual experimental data. The final section summarizes conclusions.

2. MULTILAYER FEEDFORWARD NEURAL NETWORKS

The multilayer feedforward neural network has been proven rigorously to be a universal function approximator for any bounded square integrable function of many variables.[22–24] Mathematically consider a function $\boldsymbol{\psi}: X \subseteq \mathbf{R} \rightarrow Y \subseteq \mathbf{R}$, from a bounded subset $\boldsymbol{\psi}(X)$ of $\mathbf{R}^n$ to a bounded subset of $\mathbf{R}^m$ where the function is unknown but is assumed to be in L^2. Given sufficient input–output data $[\mathbf{x}_i, \boldsymbol{\psi}(\mathbf{x}_i)]$, often called as training patterns or training data, the neural network, as an approximation function, $\hat{\boldsymbol{\psi}}: X \subseteq \mathbf{R} \rightarrow Y \subseteq \mathbf{R}^m$, is determined by the well-known backpropagation algorithm as if the objective

$$\min_{\hat{\boldsymbol{\psi}}} \sum_i \| \hat{\boldsymbol{\psi}}(\mathbf{x}_i) - \boldsymbol{\psi}(\mathbf{x}_i) \|^2 \tag{1}$$

were achieved where $\mathbf{x}_i \in \mathbf{R}^n$ is the input to the function. The network is then used for feedforward computation with various inputs. Such training of the network is normally depicted by the block diagram shown in Figure 1.

The schematic diagram of the internal structure of the neural network is shown in Figure 2. The network consists of the input layer, hidden layers and output layer, each having a number of

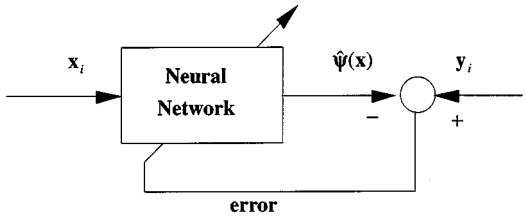

Figure 1. Training of neural network

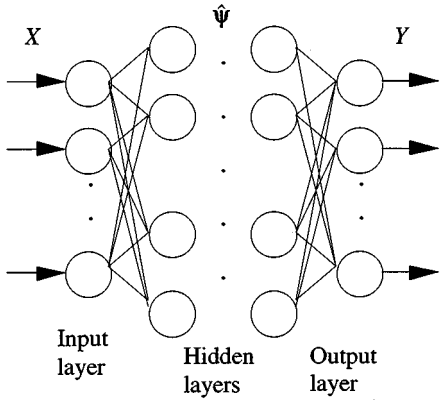

Figure 2. Multilayer feedforward neural network

units, depicted as circles. Each unit is connected to units in the neighbouring layer with a weight, shown as a line in the figure. The actual neural network is thus parametrized by a set of weights W, and in conventional backpropagation training, the objective substantially turns out to be

$$\min_{W} \sum_{i} \|\hat{\boldsymbol{\psi}}(\mathbf{x}^0; W) - \boldsymbol{\psi}(\mathbf{x}^0)\|^2 \tag{2}$$

where $\mathbf{x}^0 = \mathbf{x}_i$ is the input to the network while $\hat{\boldsymbol{\psi}}(\mathbf{x}^0; W) = \mathbf{x}^K = \mathbf{y}^i \in \mathbf{R}^n$ is the output, represented by a K layer network. The input and output of the network are computed by the recursive relationship

$$\mathbf{y}^j = \mathbf{W}^j \mathbf{x}^{j-1} + \mathbf{v}^j \tag{3}$$

$$\mathbf{x}^j = (v(\mathbf{y}_1^j), v(\mathbf{y}_2^j), \ldots, v(\mathbf{y}_{n_j}^j)) \tag{4}$$

for $j = 1, 2, \ldots, K$, where n_j is the dimension of the vectors $\mathbf{y}^j$ and $\mathbf{x}^j$, and $\mathbf{y}_i^j$ denotes the ith component of $\mathbf{y}^j$. The scalar functions $v(.)$ are monotonically increasing threshold functions, e.g.

$$v(.) = \tanh(.) \tag{5a}$$

or

$$v(.) = \frac{1}{1 + e^{(.)}} \tag{5b}$$

Let W denote the set of weight parameter matrices/vectors $W = \{\mathbf{W}^1, \mathbf{W}^2, \ldots, \mathbf{W}^K; \mathbf{v}^1, \mathbf{v}^2, \ldots, \mathbf{v}^K\}$.

The derivation of the gradient of $\hat{\boldsymbol{\psi}}(\mathbf{x}^0; W)$ with respect to the individual synaptic weights W_{ij}^k and v_i^k is essentially given by the well-known backpropagation formula.[25] For the output (Kth) layer,

$$\frac{\partial x_\alpha^K}{\partial W_{ij}^K} = \theta_{\alpha i}^K x_j^{K-1} \tag{6a}$$

$$\frac{\partial x_\alpha^K}{\partial v_i^K} = \theta_{\alpha i}^K \tag{6b}$$

$$\theta_{\alpha i}^K = v'(y_i^K)\delta_{\alpha i} \tag{6c}$$

For the kth hidden layer ($k = K-1, K-2, \ldots, 2, 1$)

$$\frac{\partial x_\alpha^K}{\partial W_{ij}^K} = \theta_{\alpha i}^K x_j^{K-1} \tag{7a}$$

$$\frac{\partial x_\alpha^K}{\partial v_i^K} = \theta_{\alpha i}^K \tag{7b}$$

$$\theta_{\alpha i}^K = v'(y_i^K) \sum_t \theta_{\alpha i}^{k+1} W_{it}^{K+1} \tag{7c}$$

where δ_{ij} denotes the Kronecker delta tensor.

The training of the neural network through the backpropagation algorithm is iterated until a terminal condition is satisfied. Normally, input–output data which were not used for training, often termed validation data, are prepared beforehand, and the termination takes place if the mean square error in equation (2) turned unchanged through iterations.

3. MATERIAL MODELS

3.1. Elasticity and inelasticity

In engineering design and analysis, models describing stress–strain behaviour, or constitutive models, are frequently needed. Often, the stress–strain behaviour is studied by separating the effect of elastic behaviour from the overall behaviours. The total strain is thus given by the sum of the elastic strain ε^{e} and the inelastic strain $\varepsilon^{\mathrm{in}}$ under uniaxial loading condition:

$$\varepsilon = \varepsilon^{\mathrm{e}} + \varepsilon^{\mathrm{in}} \tag{8}$$

The elastic behaviour is represented by the linear relationship between the strain and stress:

$$\sigma = E\varepsilon^{\mathrm{e}} \tag{9}$$

where E is Young's modulus representing a linear coefficient.

3.2. Plasticity

Let a material be plastic for inelasticity, i.e.,

$$\varepsilon = \varepsilon^{\mathrm{e}} + \varepsilon^{p} \tag{10}$$

where ε^p is the plastic strain. Plastic hardening materials perform plastic deformations only upon increasing the stress level and the yield condition for plastic deformations changes during the loading process. The performance of such materials thus depends on the previous states of stress and strain. In such path-dependent cases, the elastic range of materials is in general expressed by means of the thermodynamic forces associated with the two internal variables, back stress representing kinematic hardening χ and drag stress representing isotropic hardening R:

$$f = J(\sigma - \chi) - R - k \leqslant 0 \tag{11}$$

where σ and k are respectively the stress and material constant, and J represents a distance in the stress space. The plastic flow follows the normality rule, which states

$$\mathrm{d}\varepsilon^{\mathrm{p}} = \mathrm{d}\lambda \frac{\partial \mathrm{f}}{\partial \sigma} \tag{12a}$$

The plastic multiplier $\mathrm{d}\lambda$ is derived from the hardening rule through the consistency condition $f = \mathrm{d}f = 0$. Materials then possesses kinematic and isotropic rules, for example

$$\mathrm{d}\chi = C\left(\frac{2}{3} a \mathrm{d}\varepsilon^{\mathrm{p}} - \chi \int |\mathrm{d}\varepsilon^{\mathrm{p}}|\right) \tag{12b}$$

$$\mathrm{d}R = b(Q - R) \int |\mathrm{d}\varepsilon^{\mathrm{p}}| \tag{12c}$$

where C, a, b and Q are material constants.[26,27] Note here that we shall not discuss the details of plastic models as they are out of scope of the paper.

3.3. *Viscoplastic models*

Materials often have viscous or time-dependent deformations. Time-independent plasticity is then considered as a particular limiting case of viscoplasticity. In the unified theory capable of describing cyclic loading and viscous behaviour,[3,28] the time-dependent effect is unified with the plastic deformations as a viscoplastic term, i.e.

$$\varepsilon = \varepsilon^{\mathrm{e}} + \varepsilon^{\mathrm{p}} + \varepsilon^{\mathrm{v}} = \varepsilon^{\mathrm{e}} + \varepsilon^{\mathrm{vp}} \tag{13}$$

where ε^{v} and $\varepsilon^{\mathrm{vp}}$ represent the viscous and viscoplastic strains, respectively.

The viscoplastic potential is generally expressed as a power function of f in equation (11). Chaboche's model,[9] a popular viscoplastic model, uses this flow rule and, under stationary temperature condition, has the form together with the kinematic and isotropic hardening rules:

$$\dot{\varepsilon}^{\mathrm{vp}} = \left\langle \frac{|\sigma - \chi| - R}{K} \right\rangle^{n} \mathrm{sgn}(\sigma - \chi) \tag{14a}$$

$$\dot{\chi} = H\dot{\varepsilon}^{\mathrm{vp}} - D\chi|\dot{\varepsilon}^{\mathrm{vp}}| \tag{14b}$$

$$\dot{R} = h|\dot{\varepsilon}^{\mathrm{vp}}| - \mathrm{d}R|\dot{\varepsilon}^{\mathrm{vp}}| \tag{14c}$$

where K, n, H, D, h, d are material parameters and $\langle . \rangle$ becomes zero if the value inside is negative. The dynamics of the equations can be uniquely specified by giving the initial conditions of

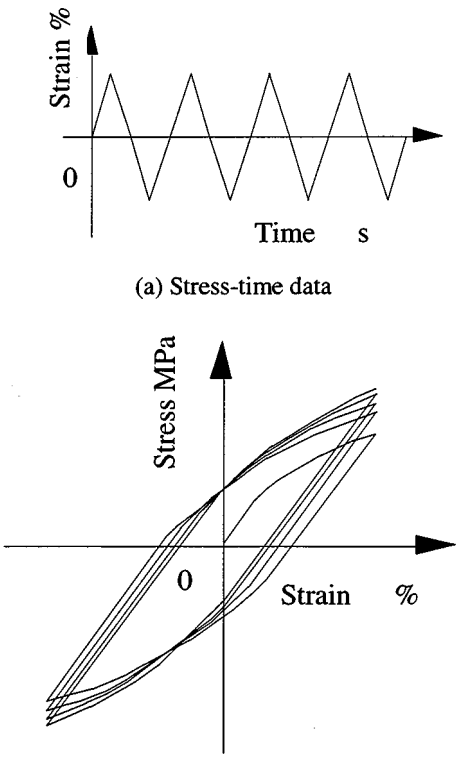

Figure 3. Reverse cyclic loading test

the variables:

$$\varepsilon^{\mathrm{vp}}|_{t=0} = \varepsilon_0^{\mathrm{vp}} \tag{15a}$$

$$\chi|_{t=0} = \chi_0 \tag{15b}$$

$$R|_{t=0} = R_0 \tag{15c}$$

In the case of reverse cyclic loading with constant strain limits and rates as shown in Figure 3(a), which is of concern in the paper, we know the initial condition of strain

$$\varepsilon|_{t=0} = \varepsilon_0 \tag{16}$$

and the strain rate

$$\dot{\varepsilon} = \begin{cases} \dot{\varepsilon}_c & \text{for } 2nt_c \leqslant t < (2n+1)t_c \\ -\dot{\varepsilon}_c & \text{for } (2n+1)t_c \leqslant t < 2(n+1)t_c \end{cases}, \quad n = 0, 1, 2, \ldots \tag{17}$$

These first allow us to know the time history of strain ε iteratively

$$\varepsilon_{k+1} = \varepsilon_k + \Delta t \cdot \dot{\varepsilon}_k \tag{18}$$

The initial stress is thus derived from equations (9), (10), (15a) and (16)

$$\sigma|_{t=0} = E(\varepsilon_0 - \varepsilon_0^{\mathrm{vp}}) \tag{19}$$

The next states of the viscoplastic strain, back stress and drag stress can be then derived after their rate of change has been computed by equations (14):

$$\varepsilon_{k+1}^{\mathrm{vp}} = \varepsilon_k^{\mathrm{vp}} + \Delta t \cdot \dot{\varepsilon}_k^{\mathrm{vp}} \tag{20a}$$

$$\chi_{k+1} = \chi_k + \Delta t \cdot \dot{\chi}_k \tag{20b}$$

$$R_{k+1} = R_k + \Delta t \cdot \dot{R}_k \tag{20c}$$

We can also derive the next state of stress σ_{k+1} through equations (18) and (19a):

$$\sigma_{k+1} = E(\varepsilon_{k+1} - \varepsilon_{k+1}^{\mathrm{vp}}) \tag{21}$$

and the repetition of these operations enables us to carry out the whole computer simulation. The stress–strain curve, general input–output data used to show the performance of material constitutive models is shown in Figure 3(b).

Chaboche's model explained here is suited for inelastic material characteristics in a wide range as one of the best models although is not very appropriate to describe the tensile behaviour. Needless to say, other conventional models also have advantages and disadvantages, and this is largely due to the fact that the descriptive capability of models depends on their explicit mathematical formulation. The next section will present the definition of implicit material models and a model based on neural networks.

4. NEURAL CONSTITUTIVE MODELLING

4.1. Explicit and implicit constitutive models

Having a look at conventional constitutive models described in the last section, we can define explicit and implicit constitutive models as follows:

Definition (*Explicit constitutive models*). Let $\mathbf{x}$ and $\mathbf{a}$ be a set of variables and material parameters respectively and $\boldsymbol{\phi}$ the model equations. Note here that $\mathbf{x}$ includes both the input and output variables. In the case of material models, input variables are viscoplastic strain $\varepsilon^{\mathrm{vp}}$ and material internal variables $\boldsymbol{\xi}$, and the output variable is σ. Explicit constitutive models are then given by

$$\boldsymbol{\phi}(\mathbf{x}; \mathbf{a}) = \mathbf{0} \tag{22}$$

where $\boldsymbol{\phi}$ has an explicit expression.

Definition (*Implicit constitutive models*). In implicit constitutive models, model equations $\boldsymbol{\phi}$ ideally have no explicit expressions:

$$\boldsymbol{\phi}(\mathbf{x}) = \mathbf{0} \tag{23}$$

thus containing no material parameters. Implicit constitutive models are henceforth constructed only from the input–output data without any analytical investigations.

Conclusively, the advantage of explicit constitutive models is that they can be easily developed if their mechanics are clear. On the other hand, implicit constitutive models have their potential if their mechanics are unknown but input–output data are obtainable. The important thing here is hence the selection of input and output variables. The next section will deal with the selection by representing viscoplastic constitutive models in a state space form.

4.2. State-space representation of viscoplastic constitutive models

The idea of state space comes from the state-variable method of describing differential equations. In this method, dynamical systems are described by a set of first-order differential equations in variables called the state, and the solution may be visualized as a trajectory in space.

Use of the state-space approach has been often referred to as modern control theory,[29] whereas use of transfer-function-based methods such as root locus and frequency response have been referred to as classical control design. Advantages of state-space design are especially apparent when engineers design controllers for systems with more than one control input or more than one sensed output. A further advantage of the state-space design is that the system representation provides a complete (internal) description of the system, including possible internal oscillations or instabilities that might be hidden by inappropriate cancellations in the transfer-function (input/output) description.

The motion of any finite dynamical system can be expressed as a set of first-order ordinary differential equations. This is often referred to as the state-variable representation. In general, a nonlinear dynamic system is given by

$$\dot{\mathbf{x}} = \boldsymbol{\psi}(\mathbf{x}, \mathbf{u}; \mathbf{a}) \tag{24a}$$

with initial conditions:

$$\mathbf{x}|_{t=0} = \mathbf{x}_0 \tag{24b}$$

where $\mathbf{x} \in R^n$ is a set of n variables and $\mathbf{u} \in R^r$, known for all t, is a set of r control inputs. $\boldsymbol{\psi} : R^n \times R^r \to R^n$ is assumed to be continuously differentiable with respect to each of its arguments.

For example, Newton's law for a single mass M moving in one dimension x under force F is

$$M\ddot{x} = F \tag{25}$$

If we define one state variable as the position $x_1 = x$ and the other state variable as the velocity $x_2 = \dot{x}$, this equation can be written as

$$\dot{x}_1 = x_2 \tag{26a}$$

$$\dot{x}_2 = \frac{F}{M} \tag{26b}$$

These first-order linear differential equations can be concisely expressed using matrix notation. If we collect the state into a column vector $\mathbf{x}$, and the coefficients of the state equations into a square matrix $\mathbf{A}$, and the coefficients of the input into the column matrix $\mathbf{B}$, these equations can be written in matrix form as

$$\begin{bmatrix} \dot{x}_1 \\ \dot{x}_2 \end{bmatrix} = \begin{bmatrix} 0 & 1 \\ 0 & 0 \end{bmatrix} \begin{bmatrix} x_1 \\ x_2 \end{bmatrix} + \begin{bmatrix} 0 \\ 1/M \end{bmatrix} F \tag{27a}$$

or

$$\dot{\mathbf{x}} = \mathbf{A}\mathbf{x} + \mathbf{B}u \tag{27b}$$

where $\mathbf{A}$ is the system matrix and $\mathbf{B}$ is the input matrix. More generally the equation is hence represented by equation (24a). The dynamics of the system is uniquely determined if the initial state of the state variables is given:

$$\mathbf{x}|_{t=0} = \mathbf{x}_0 \tag{28}$$

In sanction with the state-space method, so as to describe dynamics or viscoplasticity in constitutive models, explicit models are thus defined with the explicit equations $\boldsymbol{\psi}$:

$$\dot{\mathbf{x}} = \boldsymbol{\psi}(\mathbf{x}, \mathbf{u}; \mathbf{a}) \tag{29}$$

Meanwhile, implicit viscoplastic constitutive models are expressed with implicit mapping $\boldsymbol{\psi}$:

$$\dot{\mathbf{x}} = \boldsymbol{\psi}(\mathbf{x}, \mathbf{u}) \tag{30}$$

4.3. Generalization of viscoplastic constitutive models and neural network constitutive models

The state-space representation of viscoplastic models described in the last section renders us possible to construct the viscoplastic constitutive models in a general fashion. Let the viscoplastic strain, internal variables, stress and material parameters be $\varepsilon^{\mathrm{vp}}$, $\boldsymbol{\xi}$, σ and $\mathbf{a}$ respectively, the generalized form of explicit constitutive model may be written as

$$\dot{\varepsilon}^{\mathrm{vp}} = \hat{\dot{\varepsilon}}^{\mathrm{vp}}(\varepsilon^{\mathrm{vp}}, \boldsymbol{\xi}, \sigma; \mathbf{a}) \tag{31a}$$

$$\dot{\boldsymbol{\xi}} = \hat{\dot{\boldsymbol{\xi}}}(\varepsilon^{\mathrm{vp}}, \boldsymbol{\xi}, \sigma; \mathbf{a}) \tag{31b}$$

It can be seen that a number of existing explicit models have similar representations. The generalized implicit constitutive model can thus have the form

$$\dot{\varepsilon}^{\mathrm{vp}} = \hat{\dot{\varepsilon}}^{\mathrm{vp}}(\varepsilon^{\mathrm{vp}}, \boldsymbol{\xi}, \sigma) \tag{32a}$$

$$\dot{\boldsymbol{\xi}} = \hat{\dot{\boldsymbol{\xi}}}(\varepsilon^{\mathrm{vp}}, \boldsymbol{\xi}, \sigma) \tag{32b}$$

Note here that internal variables can be the back and drag stresses or anything else, depending on material behaviour to be described.

Considering the state-space method, we can find that the viscoplastic strain and internal material variables correspond to the state variables whereas the stress acts as a control input. The dynamics of the models can be hence uniquely specified by giving the initial conditions of the state variables:

$$\varepsilon^{\mathrm{vp}}|_{t=0} = \varepsilon_0^{\mathrm{vp}} \tag{33a}$$

$$\boldsymbol{\xi}|_{t=0} = \boldsymbol{\xi}_0 \tag{33b}$$

and the control input σ for all t. The viscoplastic strain and internal variables can be simulated through the discretised integration scheme:

$$\varepsilon_{k+1}^{\mathrm{vp}} = \varepsilon_k^{\mathrm{vp}} + \Delta t \cdot \dot{\varepsilon}_k^{\mathrm{vp}} \tag{34a}$$

$$\boldsymbol{\xi}_{k+1} = \boldsymbol{\xi}_k + \Delta t \cdot \dot{\boldsymbol{\xi}}_k \tag{34b}$$

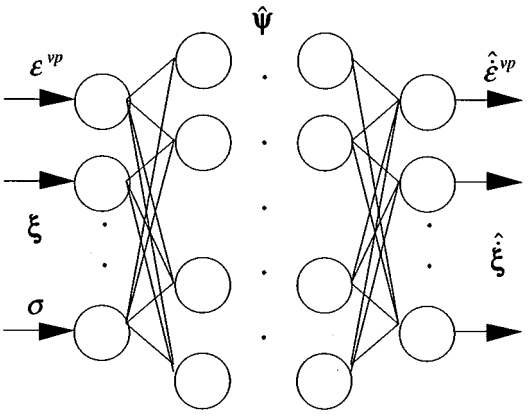

Figure 4. Proposed neural network constitutive model

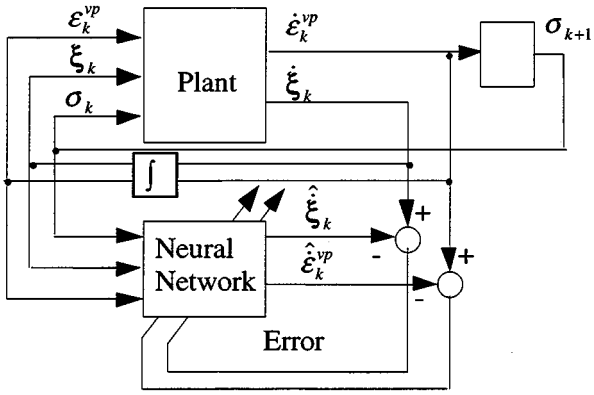

Figure 5. Training of the proposed model

Control inputs of dynamical systems should be known for all t *a priori*, normally being independent of the state variables, but the control input of the viscoplastic material is the stress and is therefore derived from the state variables iteratively, i.e. the next state of stress σ_{k+1} can be derived from the current stress σ_k, first computing the initial stress:

$$\sigma|_{t=0} = E(\varepsilon_0 - \varepsilon_0^{\mathrm{vp}}) \tag{35a}$$

$$\sigma_{k+1} = \varphi(\sigma_k) \tag{35b}$$

The derivation of σ_{k+1} is explained in Section 3.3.

In accordance to the fact that state space forms in various applications have been successfully learned by neural networks,[30–32] we propose a neural network constitutive model where the neural network learns the mapping $\hat{\dot{\varepsilon}}^{\mathrm{vp}}$ and $\hat{\dot{\xi}}$. The architecture of the proposed model is shown in Figure 4. The model inputs the current viscoplastic strain, internal variables and stress, outputting the current rate of change of viscoplastic strain and internal variables. As an example, if two

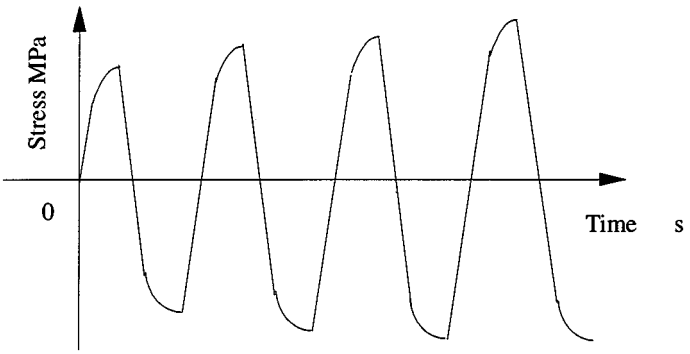

Figure 6. Stress–time curve

internal variables of back and drag stresses are chosen as in Chaboche's model, the proposed model is composed of four inputs and three outputs. The block diagram for training the model is illustrated in Figure 5.

The superiority of the proposed model to all the explicit models may be summarised by the following four facts. First, because of the implicitness, the proposed model can deal with a broad range of material behaviour. Secondly, one only needs to choose state variables to construct the proposed model unlike all the explicit models where tedious trial-and-error processes for their formulation are necessary as the implicit model can be constructed only from input–output data. Thirdly, the proposed model has the state space representation, thus capable of describing any dynamical behaviours of materials. Fourthly, since an excellent universal function approximator of neural network is used, the proposed model can create very accurate material behaviours.

4.4. Derivation of training data

While the experimental data usually describe only stress–strain relationships and their time histories, training the proposed model requires different information, i.e. the values of inelastic strain, internal variables and stress at every iterative time step for inputs ε^{vp}, ξ, σ and the values of rate of inelastic strain and internal variables at the step for outputs $\dot{\varepsilon}^{vp}$, $\dot{\xi}$. Information sufficient for training the network becomes henceforth the time histories of the inelastic strain, internal variables and stress, so that they must be extracted from experimental data.

Difficulty in extracting such training data from experiments stems from non-phenomenological characteristics of internal variables, i.e. the concept of the variables is simply rooted in the theory of inelasticity (plasticity), as was described in Section 3, rather than obtainable experimental information. The difficulty can however be overcome by taking data which well characterises internal variables. Although various internal variables can be considered depending on which material phenomena to be achieved, a technique for the decomposition proposed here is in conjunction with kinematic and isotropic hardening variables as they are of our interest.

Given experimental data *a priori* in case of the reversed cyclic loading shown in Figure 3, the training data are obtained in the following order:

(1) draw the stress–time curve shown in Figure 6 from the stress–strain and strain–time curves,

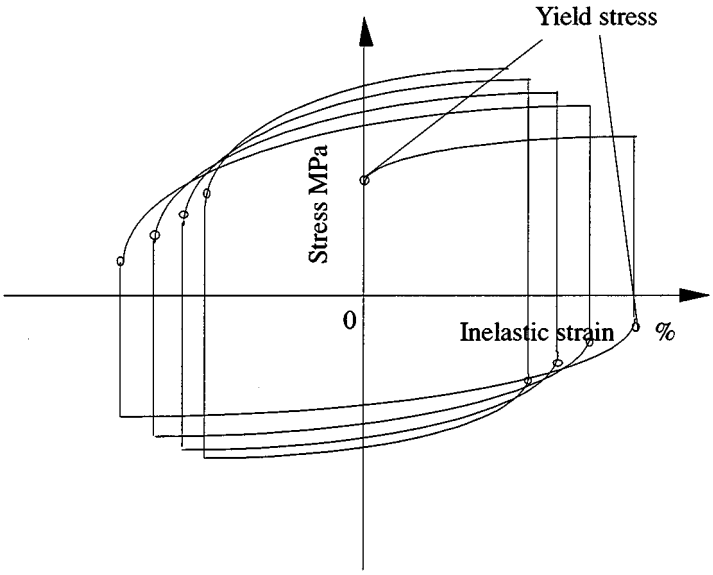

Figure 7. Stress–inelastic strain curve

(2) estimate the Young's modulus from the stress–strain curve and eliminate the stress–elastic strain component from the stress–strain curve to obtain the stress–inelastic strain curve as shown in Figure 7,
(3) draw the inelastic strain–time curve by combining the stress–time and stress–inelastic strain curves as illustrated in Figure 8,
(4) plot the absolute values of each yield stress with respect to the absolute value of inelastic strain from the stress–inelastic strain curve and interpolate linearly between the adjacent plots as shown in Figure 9,
(5) draw a stress–time curve by incorporating the inelastic strain–time curve to get the time history of the isotropic hardening stress as can be seen in Figure 10,
(6) subtract the total stress from the isotropic hardening stress with respect to time to obtain the kinematic hardening stress–time curve depicted in Figure 11,
(7) prescribe a time interval and obtain the states and increments of the inelastic strain, kinematic and isotropic stresses as well as the total stress from Figures 6, 10, and 11 at every interval.

5. NUMERICAL EXAMPLES

5.1. Ability to replace explicit constitutive models

In this section, the performance of the proposed model is investigated using pseudo–experimental data created from Chaboche's model. Shown in Figure 12 are the equations that the proposed model should learn. Non-linearity of equation (14), including $\langle\cdot\rangle$ and $|\cdot|$, obviously renders the proposed model difficult to learn the equations.

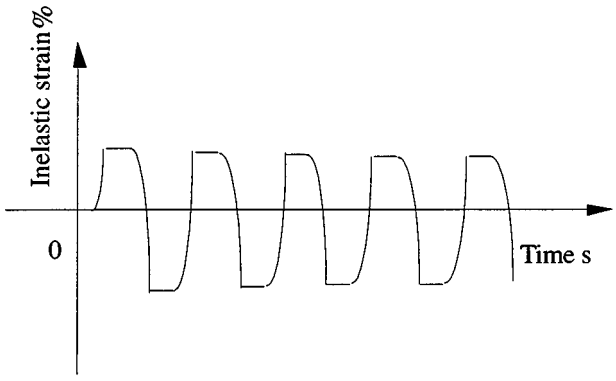

Figure 8. Inelastic strain–time curve

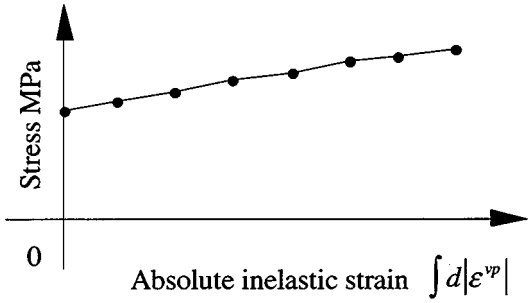

Figure 9. Yielding stress with respect to inelastic strain

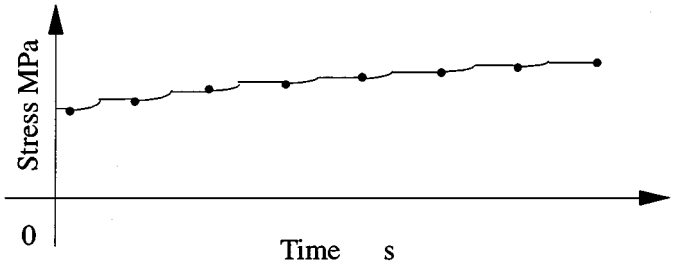

Figure 10. Isotropic hardening stress–time curve

Material parameters used to create training and validation data are listed in Table I. The number of training data were 307, and they were regularly taken from the first five cycles of a reverse cyclic loading test with a constant strain rate, parameters of which are listed in Table II. Each validation data was plotted in the center of two neighbouring training data. The stress–strain representation of the training data and validation data is indicated in Figure 13(a),

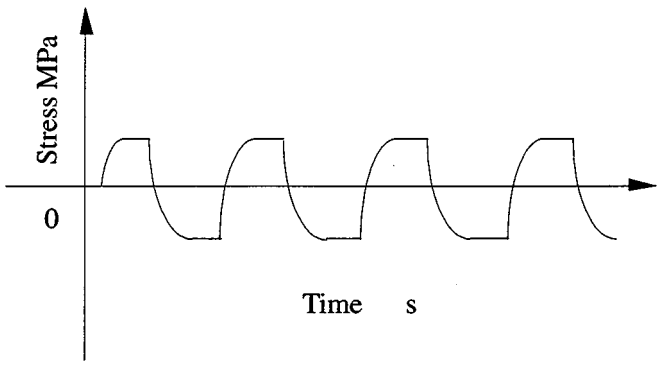

Figure 11. Kinematic hardening stress–time curve

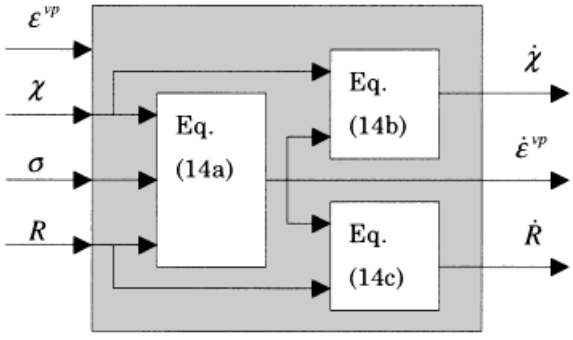

Figure 12. Equations to learn for the proposed model

Table I. Material parameters to create training and validation data

K	n	H	D	H	R_0	d
50	3	5000	100	300	50	0·6

Table II. Parameters of the reverse cyclic loading test

ε_{max} (per cent)	$\lvert\dot{\varepsilon}\rvert$ (per cent/s)	No. of training sets	No. of validation sets
0·036	$8{\cdot}0 \times 10^{-3}$	307	306

whilst Figures 13(b) and 13(c) show the strain and stress training data with respect to time, respectively. Two hidden layers each with six units were placed between the input and output layers. All processes necessary for neural networks were conducted using free software Stuttgart Neural Network Simulator (SNNS), developed by University of Stuttgart.

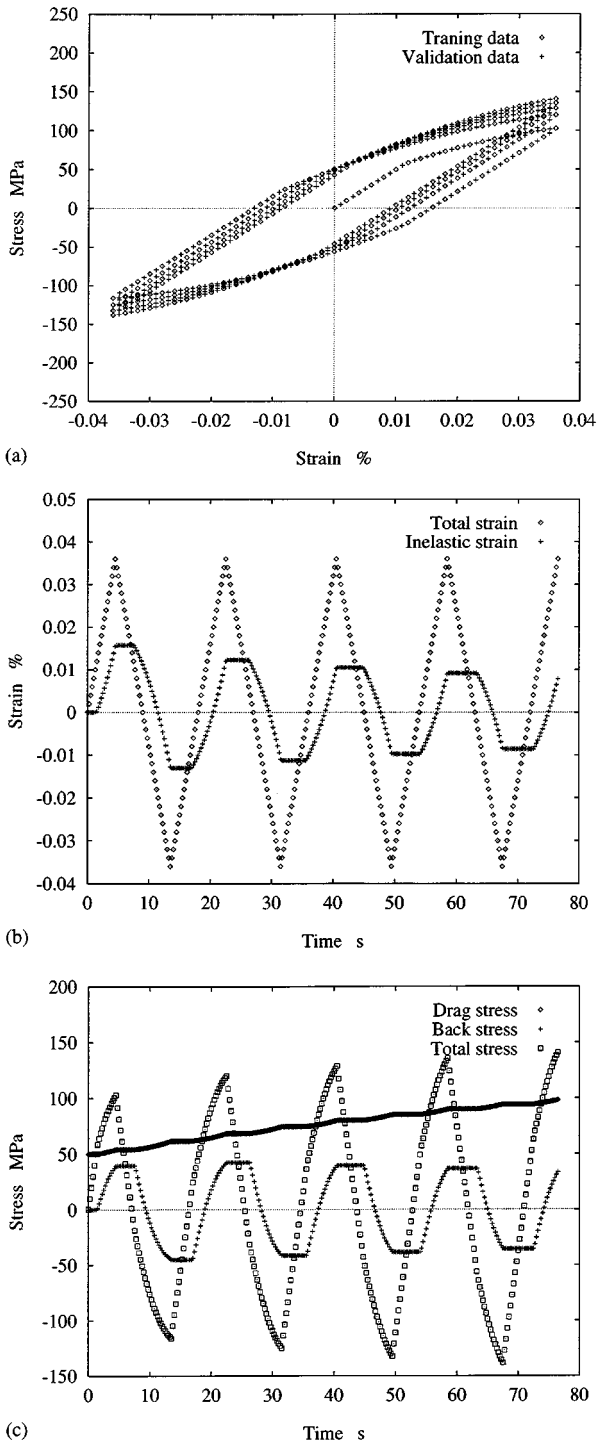

Figure 13. Training data created by Chaboche's model: (a) stress–strain data; (b) strain data; (c) stress data

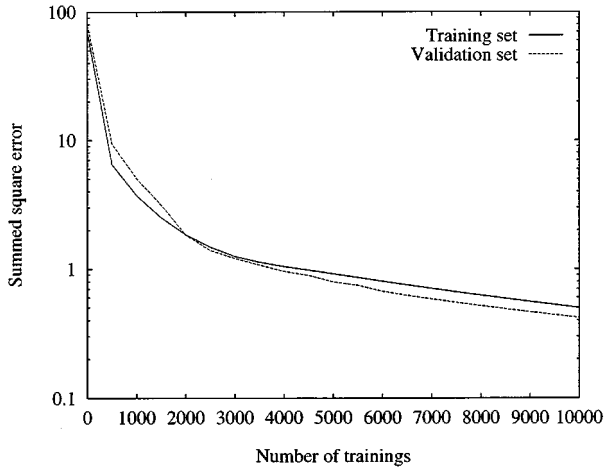

Figure 14. Error development during training

The error development of the training and validation sets until 10,000 training iterations is shown in Figure 14. Clearly, the error is approaching to zero, indicating that the neural network is learning the material model. Figure 15 shows strain–time, stress–time and stress–strain training data and the corresponding curves created by the neural network. It is seen that the curves well correlate with the training data, indicating that the model can mimic Chaboche's model.

Now that we found that the proposed model could reproduce the training data, we investigated the ability of the model to produce untrained curves. The performance of the model with cyclic strain ranges of $\pm 0{\cdot}025$, $\pm 0{\cdot}040$ and $\pm 0{\cdot}072$ per cent were simulated and compared to the exact curves by Chaboche's model.

Figure 16 show the strain–time, stress–time and stress-strain curves by the proposed method with $\pm 0{\cdot}025$ per cent strain range. The proposed model has a good agreement with the exact curve. This is found due to the ability of interpolation of the neural network. For example, at the maximum strain of the first cycle of the training data, the drag and back stresses are 55·3 and 43·4 MPa, respectively, whereas the corresponding curve by the proposed model has a drag stress of 51·7 MPa ($< 55{\cdot}3$ MPa) and a back stress of 26·2 MPa ($< 43{\cdot}4$ MPa), and the curve by the proposed model is within the training data all the time.

A similar material behaviour to the exact curve by Chaboche's model is obtained with $\pm 0{\cdot}040$ per cent as shown in Figure 17, though the range exceeds that of the training data. This result indicates that the proposed model can create a curve similar to the exact curve extrapolatively if the extrapolation is adjacent. However the peak of the second cycle of back stress shows large errors, indicating that there is no guarantee in extrapolation.

The curves of the proposed model with $\pm 0{\cdot}072$ per cent are far off the exact curves as illustrated in Figure 18. We can clearly see that the curve by the proposed model in the first cycle deviated from Chaboche's curve after a strain of 0·036 per cent, which the proposed model did not experience for training. There exist considerable errors in stress and strain curves.

5.2. Ability to replace experimental data

The proposed model was applied to the actual experimental data of 2 1/4Cr-1 Mo Steel under a temperature of 673 K, obtained from a benchmark project by the Society of Material Science,

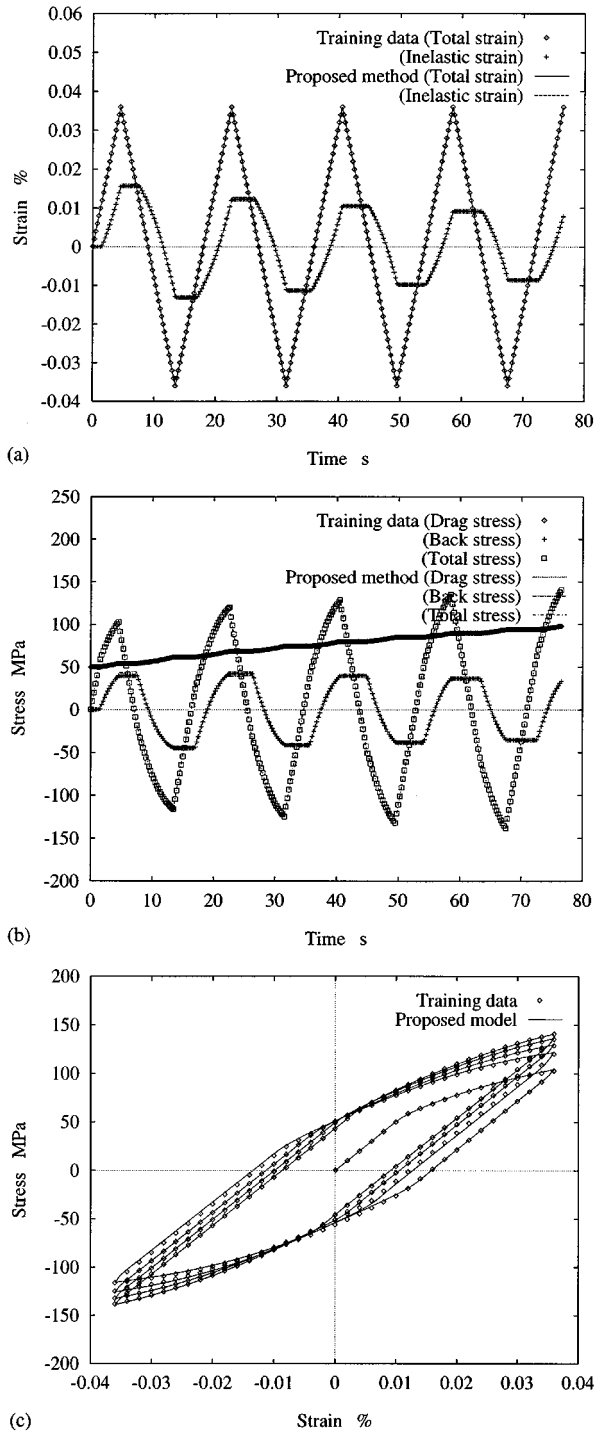

Figure 15. Training data and corresponding curve created by the proposed model: (a) strain-time data; (b) stress-time data; (c) stress–strain data

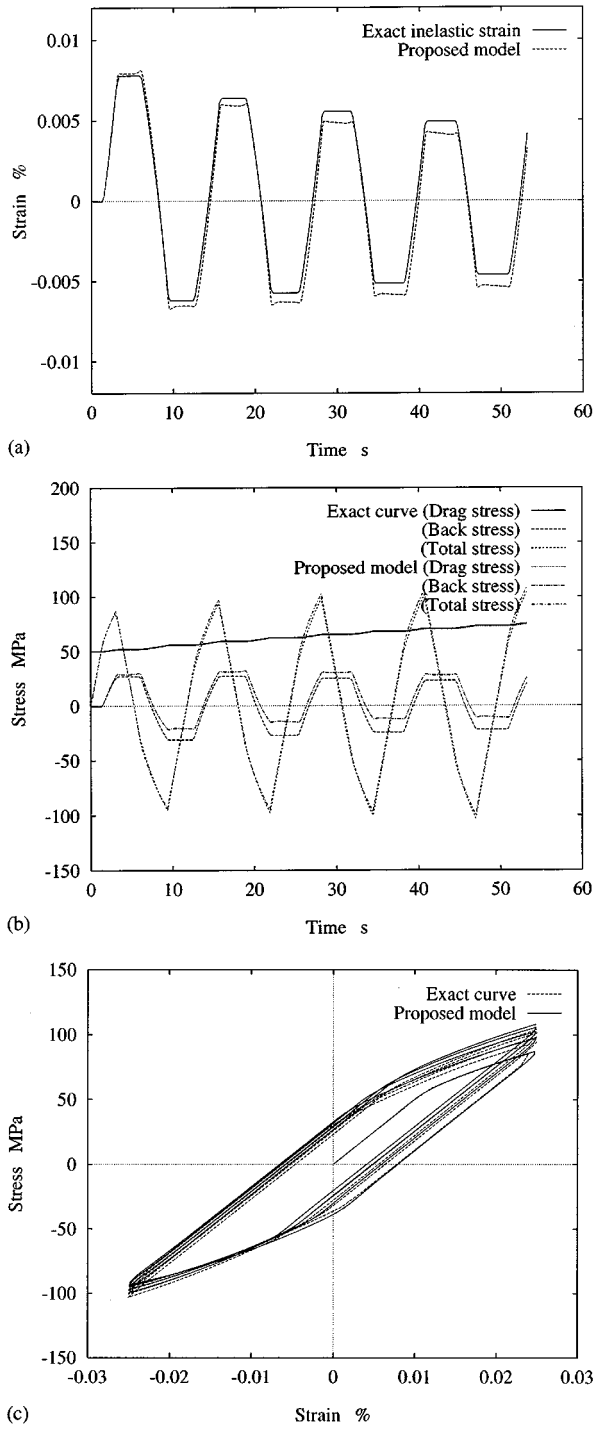

Figure 16. Performance of the proposed model with maximum strain range 0·025 per cent: (a) strain-time curve; (b) stress-time curve; (c) stress–strain curve

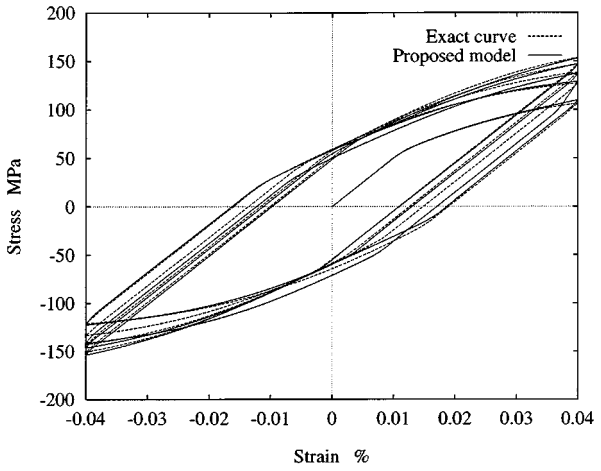

Figure 17. Performance of the proposed model with maximum strain range 0·040 per cent

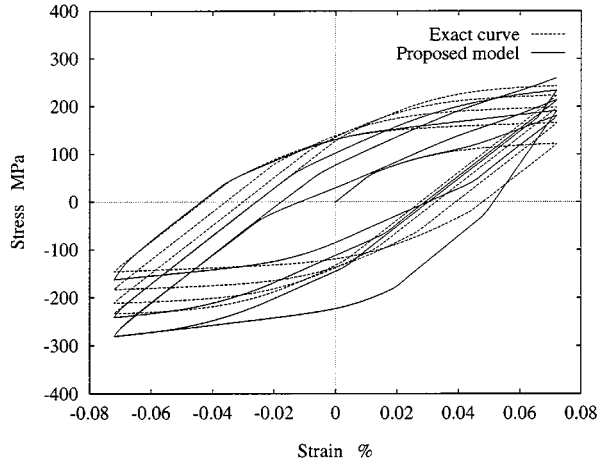

Figure 18. Performance of the proposed model with maximum strain range 0·072 per cent

Japan.[33] Experimental data used included stress–strain data with strain rates of 0·0001, 0·01 and 0·5 per cent/s, and they are shown in Figure 19. For simplicity, the proposed model was used to learn data with only one strain rate at a time. As an example, Figure 20 depicts the time histories of first cycles of the inelastic strain, isotropic and kinematic hardening stresses and total stress with a strain rate of 0·5 per cent/s. Training data with different cycles and strain rates were also prepared in the same manner. The model used here had the same architecture as the one described in Section 4.3, and the technique explained in Section 4.4 was used to extract training data for the proposed model from experimental data. As the explicit constitutive model for comparison, the performance of Chaboche's model, parameters of which were

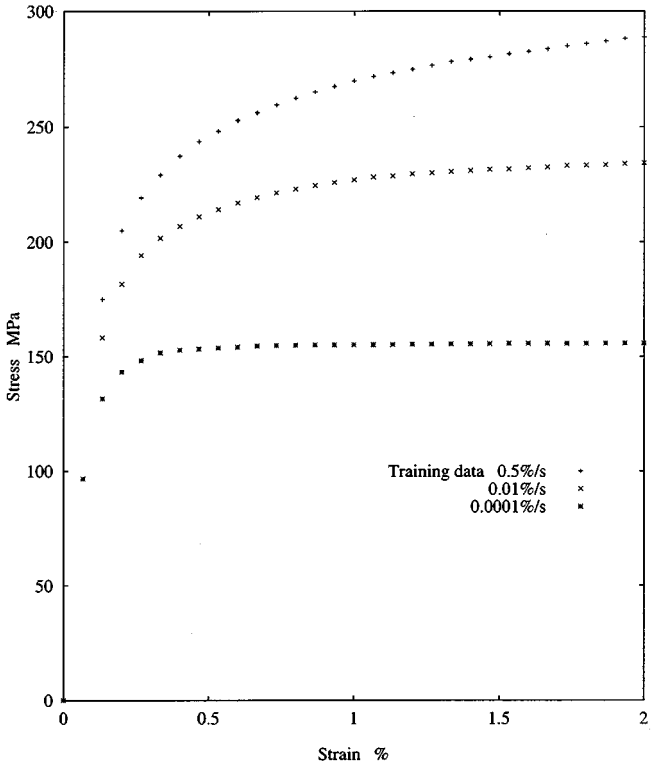

Figure 19. Experimental data of 2 1/4Cr-1 Mo steel

best fitted by a parameter identification technique[34] through all the strain rates, was also investigated.

Figure 21 shows curves each created by the resultant model, together with the corresponding training data, after 20,000 training iterations were completed. Although direct comparison cannot be made due to the fact that neural networks were each used to learn only one curve, it is seen that, in comparison to the best-fit Chaboche's curve in Figure 22, the configuration of the proposed model is significantly similar to the experimental data.

6. CONCLUSIONS

The implicit constitutive model has been defined and an implicit viscoplastic model using neural networks has been proposed in this paper. The proposed model, based on the state-space method, has the inputs of the current viscoplastic strain, internal variables and stress and the outputs of the current rates of change of the viscoplastic strain and material internal variables.

The proposed model was trained using input–output data generated from Chaboche's model, and could reproduce the original stress–strain curve. In addition, the model demonstrated the ability of interpolation by generating untrained curves. It was also found that the model can extrapolate in close proximity to the training data although it is not extrapolatively precise to

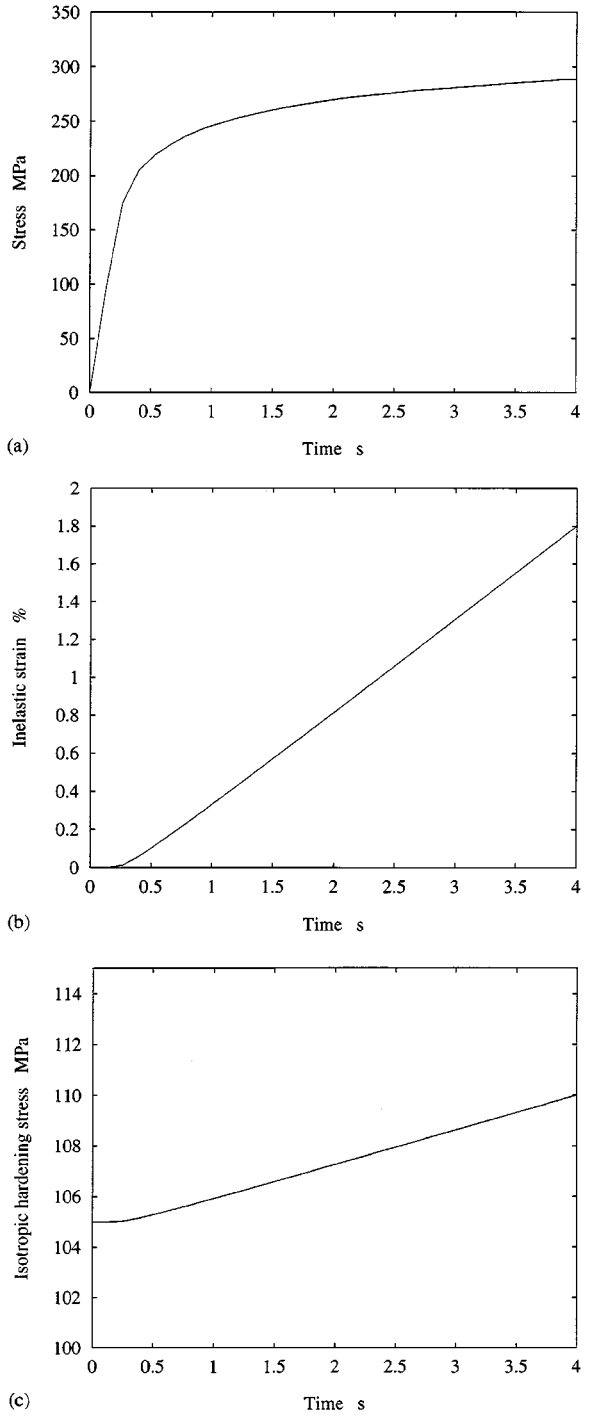

Figure 20. Training data of the first cycle with 0·5 per cent/s: (a) stress-time curve; (b) inelastic strain-time curve; (c) isotropic hardening stress–time curve; (d) kinematic hardening stress-time curve

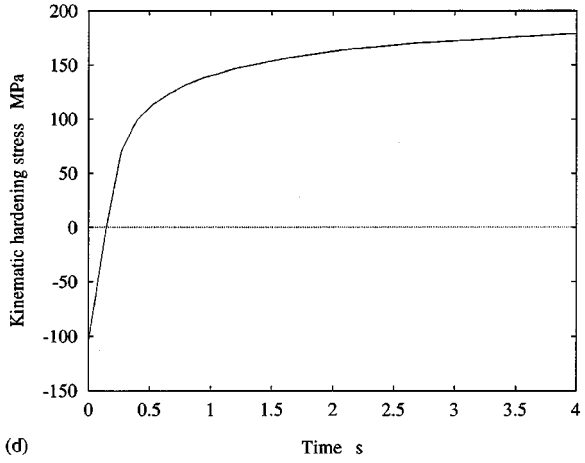

Figure 20. (*Continued*)

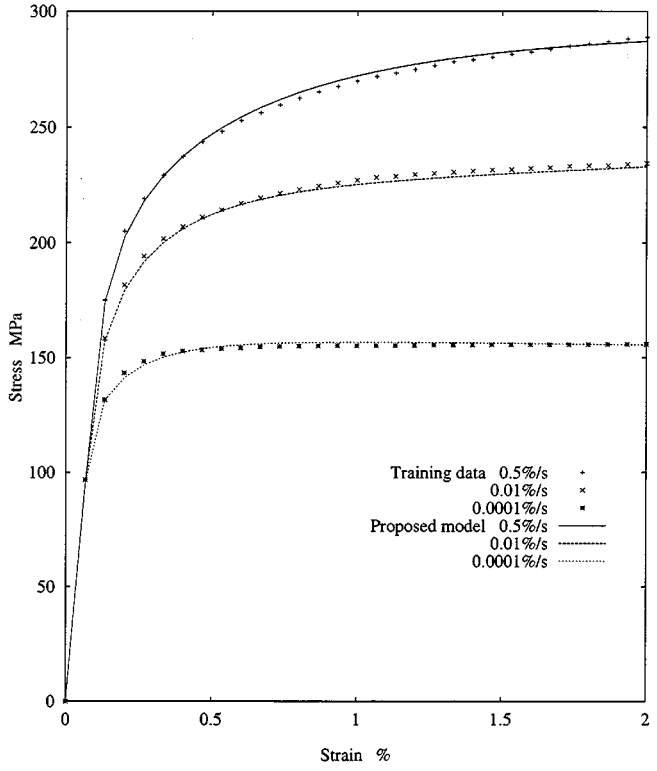

Figure 21. Performance of the proposed model and experimental data

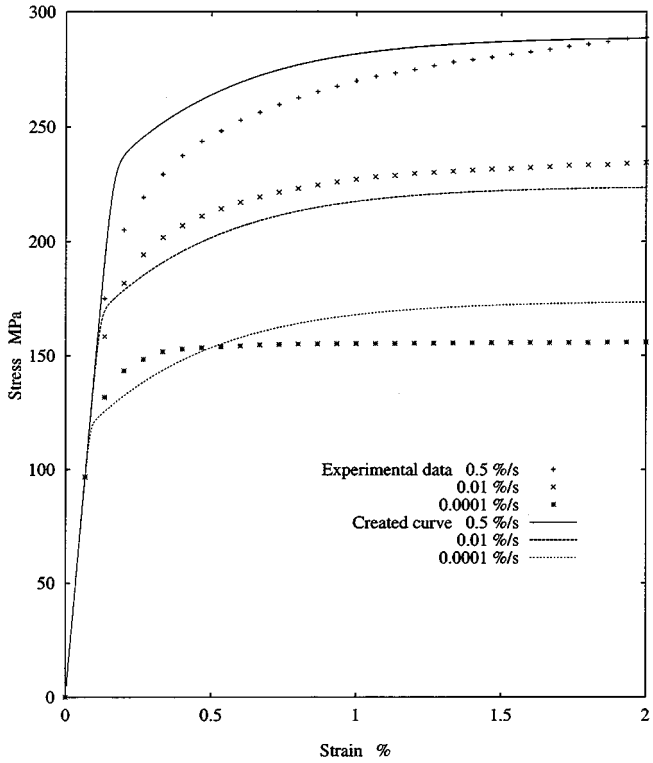

Figure 22. Performance of the best fit Chaboche's model and experimental data

a large extent. Therefore, the proposed model can replace Chaboche's model completely by its interpolative capability if a variety of training data with different conditions are used. A simple technique to derive training data for the proposed model from experimental data was also described. Having been tested with the actual experimental data, the proposed model could correlate well with material behaviours in comparison to the best fit Chaboche's model. In conclusion, the results of the numerical examples obviously indicates the superiority of the proposed model to all the existing explicit constitutive models, at least in an interpolative fashion.

The paper was mainly aimed at describing the concept of the proposed model as the first step, thereby indicating its applicability only from simple experimental data, so various further studies are still left open. Depending on the type of experiment, one may try to describe material behaviours using various characteristic points in the experiment for the representation of internal variables. Strategies for selecting proper internal variables are thus important issues. An adequate technique for extracting training data from experimental data has to be proposed for each internal variable accordingly.

Finally, the conclusive suggestion of the authors is that more researchers should be involved with implicit constitutive models as long as they have advantages over explicit models as described in the paper. At this moment, there is a big gap between implicit and explicit constitutive modelling in terms of research being carried out, i.e. only a few research projects are

ongoing with the implicit constitutive modelling in the world, while numerous researchers have been working on explicit constitutive models over decades.

REFERENCES

1. S. R. Bodner and Y. Partom, 'Constitutive equations for elastic-viscoplastic strain hardening materials', Trans. ASME, *J. Appl. Mech.*, **42,** 385–389 (1975).
2. E. W. Hart, 'Constitutive relations for the nonelastic deformation of metals', *ASME J. Eng. Mater. Technol.*, **98,** 193–203 (1976).
3. A. K. Miller, 'An inelastic constitutive model for monotonic, cyclic and creep deformation, Part I: equations development and analytical procedures, PartII: application to type 304 stainless steel', *ASME J. Eng. Mater. Technol.*, **98,** 97–107 (1976).
4. Robinson and Bartolotta, 'Viscoplastic constitutive relationship with dependence on thermomechanical history', NASA Contractor Report 174836, 1985.
5. A. D. Freed, 'Thermoviscoplastic model with application to copper', NASA TP-2845, NASA, 1988.
6. J. L. Chaboche, 'Constitutive equations for cyclic plasticity and cyclic viscoplasticity', *Int. J. Plasticity*, **5,** 247–254 (1989).
7. K. S. Chan and U. S. Lindholm, 'Inelastic deformation under nonisothermal loading', *ASME J. Eng. Mater. Technol.*, **112,** 15–25 (1990).
8. N. Ohno, 'Recent topics in constitutive modeling of cyclic plasticity and viscoplasticity', *Appl. Mech. Rev.*, **43,** 283–295 (1990).
9. J. L. Chaboche and G. Rousselier, 'On the plastic and viscoplastic equations—Part I: rules developed with internal variable concept', *Trans. ASME, J. Pressure Vessel Technol.*, **105,** 153–164 (1983).
10. W. Ramberg and W. R. Osgood, 'Description of stress-strain curves by three parameters', NACA, Technical Note, No. 902, 1943.
11. E. P. Cernocky and E. Krempl, 'A non-linear uniaxial integral constitutive equation incorporating rate effects, creep and relaxation', *Int. J. Nonlin. Mech.*, **14,** 183–203 (1979).
12. K. P. Walker, 'Representation of Hastelloy-X behavior at elevated temperature with a functional theory of viscoplasticity', ASME/PVP Century 2 Emerging Technology Conf., 1980.
13. C. G. Schmit and A. K. Miller, 'A unified phenomenological model for non-elastic deformation of type 316 stainless steel, Part I: development of the model and calculation of the material constants, Part II: fitting and predictive capabilities', *Res. Mechanica*, **3,** 109–175 (1987).
14. H. Hishida, *et al.*, 'Prediction of life time of the first wall under thermal fatigue based on viscoplastic deformations', Transactions of Seimic Isolation and Response Control for Nuclear and Non-Nuclear Structures, L, 1991, pp. 289–294.
15. G. Cailletaud and P. Pilvin, 'Identification and inverse problems related to material behavior', Inverse Problems in Engineering Mechanics, pp. 79–86, 1994.
16. R. Mahnken and E. Stein, 'Gradient-based methods for parameter identification of viscoplastic materials', Inverse Problems in Engineering Mechanics, Balkema, Rotterdam, pp. 137–144, 1994.
17. T. Furukawa and G. Yagawa, 'Parameter identification of inelastic constitutive equations using an evolutionary algorithm', Proc. 1995 ASME/JSME Pressure vessels and Piping Conf., PVP-Vol. **305,** pp. 437–444, 1995.
18. A. Gavrus, E. Massoni and J. L. Chenot, 'Constitutive parameter identification using a computer aided rheology approach', Simulation of Materials Processing: Theory, Methods and Applications, pp. 563–568, 1995.
19. J. Ghaboussi, J. H. Garrett and X. Wu, 'Knowledge-based modeling of material behavior with neural networks', *J. Mech. Division, ASCE*, **117**(1), 132–153 (1991).
20. T. Furukawa, H. Okuda and G. Yagawa, 'A neural network constitutive law based on yield and back stresses', The 8th Computational Mechanics Conf., **95-4,** 121–122 (1995).
21. T. Furukawa, H. Okuda and G. Yagawa, 'Implicit constitutive modelling using neural networks', XIXth Int. Congress of Theoret. Appl. Mech., JJ-3, 531, 1996.
22. K. Funahashi, 'On the approximate realization of continuous mapping by neural networks', *Neural Networks*, **2,** 183–192 (1988).
23. K. Hornik, M. Stinchcombe and H. White, 'Multilayer feedforward networks are universal approximators', *Neural Networks*, **2,** 359–366 (1989).
24. G. Cybenko, 'Approximation by superposition of a sigmoidal function', *Math. Control, Signal and Systems*, **2,** 303–314 (1989).
25. J. L. McClelland and D. E. Rumelhart, *Exploration in Parallel Distributed Processing*, MIT press, Cambridge, 1988.
26. P. J. Armstrong and C. O. Frederick, 'A mathematical representation of the multiaxial Bauschinger effect', C.E.G.B. Report RD/B/N 731, 1966.
27. Z. Mroz, H. P. Shriavstava and R. N. Dubey, 'A non-linear hardening model and its application to cyclic loading', *Acta Mechanica*, **25,** 51–61 (1976).

28. D. N. Robinson, C. E. Pugh and J. M. Corum, 'Constitutive equations for describing high-temperature inelastic behavior of structural alloys', Specialists meeting on High-Temperature Structural Design Technology of LMFBRs, IAEA report IWGFR/11, International Atomic Energy Agency, 1976, pp. 44–57.
29. G. F. Franklin, J. D. Powell and A. Emami-Naeini, *Feedback Control of Dynamic Systems*, Addison-Wesley, Reading, MA, 1991.
30. K. S. Narendra and K. Partharathy, 'Identification and control of dynamical systems using neural networks', *IEEE Trans*, *Neural Networks*, **1**(1), 4–27 (1990).
31. C. J. Goh, 'The neural network approach to several nonlinear control problems', Internal Report, Department of Mathematics, University of Western Australia, 1991.
32. D. H. Nguyen and B. Widrow, 'Neural networks for salf-learning control systems', *Int. J. Control*, **54**(6), 1439–1451 (1991).
33. The Society of Material Science, Japan, 'Benchmark project on inelastic deformation and life prediction of 2 1/4Cr-1 Mo Steel at high temperature under multiaxial stresses', Subcommittee on Inelastic Analysis and Life Prediction of High Temperature Materials, 1988.
34. T. Furukawa and G. Yagawa, 'Inelastic constitutive parameter identification using an evolutionary algorithm with continuous individuals', *Int. J. Numer. Meth. Engng*., **40,** 1071–1090 (1997).

